LATE: A Level Set Method Based on Local Approximation of Taylor Expansion for Segmenting Intensity Inhomogeneous Images

Hai Min, Wei Jia, Yang Zhao, Wangmeng Zuo, Haibin Ling, Yuetong Luo

***Abstract*—Intensity inhomogeneity is common in real world images and inevitably leads to many difficulties for accurate image segmentation. Numerous level set methods have been proposed to segment images with intensity inhomogeneity. However, most of these methods are based on linear approximation such as locally weighted mean, which may cause problems when handling images with severe intensity inhomogeneities. In this paper, we view segmentation of such images as a nonconvex optimization problem since the intensity variation in such an image follows a nonlinear distribution. Then, we propose a novel level set method named Local Approximation of Taylor Expansion (LATE), which is a nonlinear approximation method to solve the nonconvex optimization problem. In LATE, we use the statistical information of the local region as a fidelity term and the differentials of intensity inhomogeneity as an adjusting term to model the approximation function. In particular, since the first-order differential is represented by the variation degree of intensity inhomogeneity, LATE can improve the approximation quality and enhance the local intensity contrast of images with severe intensity inhomogeneity. Moreover, LATE solves the optimization of function fitting by relaxing the constraint condition. In addition, LATE can be viewed as a constraint relaxation of classical methods such as the Region-Scalable Fitting model (RSF) and the Local Intensity Clustering model (LIC). Finally, the level set energy functional is constructed based on the Taylor expansion approximation. To validate the effectiveness of our method, we conduct thorough experiments on synthetic and real images. Experimental results show that the proposed method clearly outperforms other solutions in comparison.**

***Index Terms*—Intensity inhomogeneity, level set, Taylor expansion, local region descriptor, nonlinear description**

Manuscript received on June 21, 2017. This work is partly supported by the grants of the National Science Foundation of China, Nos. 61702154, 61673157, the grants of Anhui Provincial Natural Science Foundation, No.1808085QF189, and also partly supported by the Fundamental Research Funds for the Central Universities, Nos. JZ2016HGBZ0803, JZ2017HGTB0189, PA2018GDQT0014, and by US National Science Foundation Grant IIS-1407156. (Corresponding author: Wei Jia)

Hai Min, Wei Jia, Yang Zhao and Yuetong Luo are with the School of Computer and Information, Hefei University of Technology, Hefei, China (Email: minhai361@aliyun.com, china.jiawei@139.com, yzhao@hfut.edu.cn, ytluo@hfut.edu.cn).

Wangmeng Zuo is with the School of Computer Science and Technology, Harbin Institute of Technology, Harbin, China (Email: cswmzuo@gmail.com).

Haibin Ling is with the Department of Computer & Information Sciences, Temple University, USA (Email: hbling@temple.edu).

I. INTRODUCTION

A. Background and Related Work

IN medical image analysis, intensity inhomogeneity usually refers to the slow, nonanatomic intensity variations of the same tissue over the image domain, which occurs in natural images as well [1-2]. In general, intensity inhomogeneity can be caused by different factors such as imperfection in the imaging device, uneven illumination, and the subject-induced susceptibility effect [3-4]. For image segmentation, intensity inhomogeneity inevitably brings many difficulties due to the overlaps among the ranges of the intensities in the regions to be partitioned. Therefore, it remains a challenging problem to accurately segment images with severe intensity inhomogeneities.

For image segmentation, level set methods are well known for capturing dynamic interfacing and shapes and have achieved state-of-the-art performance [5-8]. In these methods, the zero level set is used to represent the contours or surfaces, and it controls the curve evolving freely. A classic level set method is the Chan-Vese (CV) model [9], which seeks an approximation of a given image with a binary piecewise constant representation through a level set formulation [10]. However, due to the assumption that the images consist of statistically homogeneous regions, the CV model cannot segment images with intensity inhomogeneities well [11]. To solve the intensity inhomogeneity problem in level set methods, many new models have recently been proposed whose main idea is to fully utilize local intensity information to constrain intensity inhomogeneity [11-26, 28-31]. Generally, these models can be classified into three types, which will be introduced in the following three paragraphs.

The first type of method assumes that each local region can be described by its statistical intensity information. In this way, local regions can be further divided into object and background regions [11-17]. For example, in the Region-Scalable Fitting model (RSF) [11, 12] and the Local Image Fitting (LIF) model [14] based on the mean intensity information of local regions, different region descriptors are used to approximate local intensity to segment images. Compared with RSF, LIF improves the computational efficiency by directly defining local windows instead of computing convolution. The Local Region-Based (LRB) model [13] restricts the Dirac function in neighborhood of the zero level set, which makes the evolving curve act locally.

As a result, LRB can segment some images with intensity inhomogeneity by setting desirable initial contours and local neighborhoods. Later, to improve the segmentation performance of RSF, both the Local Gaussian Distribution (LGD) model [16] and the Local Likelihood Image Fitting (LLIF) model [17] were proposed, which utilize Gaussian distribution with different means and variations to better describe local image intensities.

In the second type of method, global intensity information and local intensity information are combined to jointly segment images with intensity inhomogeneity [18-23]. In this manner, global information is used to capture global intensity statistics to protect contour evolution from trapping in local minima, and local information is explored to eliminate the influences of intensity inhomogeneity. Specifically, Sum and Cheung [18] proposed the Global and Local (GL) model, in which the global term is derived from CV model and the local term captures the intensity variation of the weak boundary by enhancing local intensity contrast. It should be noted that the GL model utilizes only the intensity information. Different form the GL model, Wang et al. [19] proposed the United Tensor Level Set Model (UTLSM), in which multi-features of pixels, e.g., gray value and local geometrical features such as orientation and gradient, are incorporated into a three-order tensor level set model. Then, by defining a weighted distance, the final energy function is constructed in the UTLSM model. In [20], the Local Chan-Vese model (LCV) was proposed, which incorporates a local term into a global term to segment intensity inhomogeneity images. In LCV, the global term is directly derived from the CV model, and the local term is the mean information of intensity differences [20]. Specifically, in LCV, by subtracting the original image from the averaging convolution image, the intensity differences are obtained, and the contrast between foreground intensities and background intensities can be significantly enhanced [20]. In [21], an energy function is proposed by incorporating the local statistical analysis and global similarity measurement, in which the local energy term is based on the local intensity statistical analysis and the global energy term is used to minimize the Bhattacharyya distance inside and outside of the contour. In [23], the inhomogeneity of each pixel is described by its spatially nearby pixels; then, the local inhomogeneity term and global CV term are combined to segment images with intensity inhomogeneity. By further considering the global region intensity inhomogeneity, a novel level set model based on global division and adaptive scale local variation term to segment natural images is proposed in [22], in which the global intensity information and local variation information are combined to drive the contour evolution to accurately segment natural images.

In the third type, the intensity inhomogeneity representation is encoded in the level set methods to describe and construct the energy function [27]. Specifically, the intensity inhomogeneity is estimated by optimizing the energy function, and the intensity inhomogeneity image is further corrected. Based on the description formulation of the intensity inhomogeneity effect [27], Li et al. [24] proposed the Local Intensity Clustering (LIC) model, which can be regarded as a locally weighted K-means clustering method. However, LIC does not consider the clustering variance, which may cause inaccurate segmentation similar to K-means clustering based methods [25]. Zhang et al. [26] used local information based on the joint density within image patches to perform image partition. Since the pixel intensity has a multiplicative distribution structure, the maximum-a-posteriori (MAP) principle with those pixel density functions generates the model [26]. Li et al. [28] also proposed a segmentation method based on global and local image statistical information, in which the global energy based on a Gaussian model estimates the intensity distribution of the target object and background, and the local energy derived from the mutual influences of neighboring pixels can eliminate the impact of image noise and intensity inhomogeneities. Duan et al. [29] proposed a new variant of the Mumford–Shah model for simultaneous bias correction and segmentation of images with intensity inhomogeneity, in which the L0 gradient regularizer and a smooth regularizer are separately used to model the true intensity and the intensity inhomogeneity. It should be noted that aforementioned models belonging to the third type utilize local statistical information to fit or approximate the intensity distributions of object and background [24, 26, 28, 29]. Unlike these approaches, Zhang et al. [30, 31] proposed two models, *i.e.,* Maximum Likelihood in Transformed Domain Model (MLTDM) and Locally Statistical Active Contour Model (LSACM), that use Gaussian distributions with different means and variances to model objects with intensity inhomogeneity. Then, the original image intensities are mapped into the other domain so that the intensity distribution can be better separated. Considering the variance information, the LSACM [31] transforms the intensity into local region statistical information to avoid the intensity overlay in object and background regions, thereby yielding better results than LIC.

Although great progress has been made toward solving the intensity inhomogeneity problem in level set, existing methods still have some limitations. The methods of the first type describe the local region by simply using local mean information without considering the local intensity variances [11-17]. Therefore, the segmentation performances of these methods are easily influenced by the intensity inhomogeneity degree of images. For images suffering severe intensity inhomogeneities, it is difficult for these methods to produce satisfactory results. In the methods of the second type, the global and local terms are constructed separately and optimized independently, and the image intensity approximation of these methods is only a simple combination of global approximation and local approximation [18-23]. Furthermore, the methods of the third type still make a linear description or approximation of image intensity, which is denoted by the product of the intensity inhomogeneity and piecewise constant; thus, it is a challenging task for them to produce accurate segmentation results when the images are corrupted by severe intensity inhomogeneity [24-31].

B. Our Contribution

An intrinsic principle of existing level set methods is to describe the local region by defining a certain description criterion. For example, the RSF model utilizes the local weighted mean as a description criterion, and the LIC model regards the product between the intensity inhomogeneity and piecewise constant as a description criterion. In these methods, it is believed that the defined criterion can be used to accurately describe local regions located in the same object. However, this

strategy is not able to segment images with severe intensity inhomogeneities. In fact, severe intensity inhomogeneity typically implies a nonlinear distribution in intensity variation. Therefore, not all local regions can be approximated by unified linear approximation. In other words, the intensity set based on local regions is nonconvex; thus, the segmentation of a severe intensity inhomogeneity image is essentially a nonconvex optimization problem. Since a nonlinear method is a natural choice for solving nonconvex optimization problems, it is reasonable to describe a local region by nonlinear approximation. A straightforward yet effective representation for such a purpose is through the well-known Taylor expansion.

Inspired by the above discussion, we utilize Taylor expansion to relax the constraint formulation, which is equivalent to replacing the traditional description with linear approximation. The proposed method is referred to as *Local Approximation of Taylor Expansion* (LATE). LATE is built on top of local intensity statistics and differential information, which are regarded as the fidelity term and the adjusting term, respectively, and are collaborated to describe local image regions. Furthermore, we transform the adjusting term by using an intensity inhomogeneity model. Based on the model, we simplify the adjusting term and further derive the final LATE model. Integrating the above representation into the level set framework, we derive the energy functional to segment images with severe intensity inhomogeneity.

The main contributions of this work are summarized as follows:

(1) We find that segmenting images with severe intensity inhomogeneity is essentially a nonconvex optimization problem since the intensity variation of such images follows a nonlinear distribution. Existing level set models usually utilize the linear approximation to fit the nonlinear intensity distribution and are thus often ineffective. An ingredient of nonlinear approximation needs to be included to design a better fitting function.

(2) The optimal fitting function plays an important role in discriminating between object and background regions. For this purpose, we propose a nonlinear approximation method based on Taylor expansion to approximate image intensity. By using such approximation, the variation degree of intensity inhomogeneity is incorporated into local region modeling to improve the region discrimination.

(3) We propose a novel level set method named *Local Approximation of Taylor Expansion* (LATE), which solves the nonconvex optimization problem associated in our segmentation model. Utilizing Taylor expansion to construct the fitting function, LATE relaxes the constraint so that the nonconvex optimization problem can be transformed into two convex optimization problems and thus solved effectively.

(4) We show that both the RSF and LIC models can be viewed as special cases of the proposed LATE method. On the other hand, LATE can be reformulated in terms of the RSF model or LIC model.

The rest of this paper is organized as follows: Section II presents related works. Then, Section III describes the details of the proposed LATE method. The experimental validation and analysis are reported in Section IV. Finally, Section V offers concluding remarks.

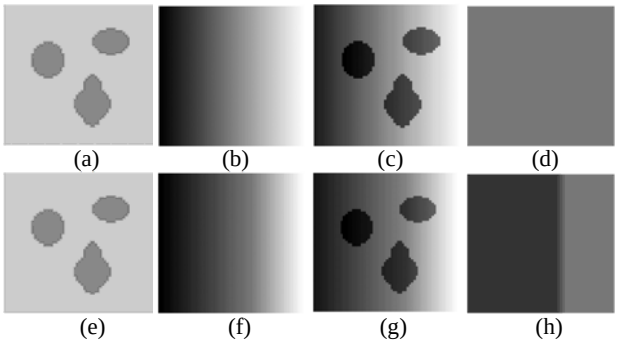

Fig.1. Variation degree of intensity inhomogeneity. (a) and (e) are original image I_0; (b) and (f) are the intensity inhomogeneities b; (c) and (g) are the intensity homogeneous images I; (d) and (h) are the variation degrees of intensity inhomogeneities.

Fig.2. Images with severe intensity inhomogeneity.

II. Background Review

In this section, we first explain the term 'severe intensity inhomogeneity.' Then, we briefly review three representative models related to our work, which are the RSF [11], LIC [24], and LSACM [31].

A. Severe Intensity Inhomogeneity

As described in [24], the input image I can be contaminated by noise and unknown intensity inhomogeneity b. The intensity inhomogeneity can be defined as the following equation:

$$I(\mathrm{y}) = b(\mathrm{y})I_0 + n \quad \textbf{(1)}$$

where b denotes the intensity inhomogeneity; I_0 is the ideal clean image, which is the "true" image before being contaminated by noise and intensity inhomogeneity, such as illumination, the device factor, and the artificial factor; the term$n$ is normally distributed with zero mean but unknown variance. Consider the simple case where the ideal image is constant C_i in each region Ω_i, and the noise n is normally zero-mean Gaussian noise and independent of those at other locations. C_i denotes the constant that is used to describe region intensity. Thus, if $\mathrm{x} \in \Omega_i$, then the intensity approximation as shown in Eq.(1) can be simplified as:

$$I(\mathrm{x}) \approx b(\mathrm{x})C_i \quad \textbf{(2)}$$

Here, the intensity inhomogeneity b is a matrix with the same dimension as image I. While all of the matrix elements of b are 1, the image is intensity homogeneous. The intensity inhomogeneity is quantified by the reference [33]. Specifically, for a 20% level, the multiplicative intensity inhomogeneity b has a range of values of 0.90 ... 1.10 over the image area. For a 40% level, the multiplicative intensity inhomogeneity b has a range of values of 0.80 ... 1.20 over the image area. For other intensity inhomogeneity levels, the field is scaled accordingly. Thus, the range of b can be regarded as [0, 2]. That is, the intensity inhomogeneity is quantified by computing the

variation of b in the whole image. The variation degree of intensity inhomogeneity is the variation of b in the local region of image.

Then, we define the variation degree of intensity inhomogeneity as the range b in a local region with fixed size: $max_{\mathrm{x}\in\Omega_\mathrm{y}} b(\mathrm{x}) - min_{\mathrm{x}\in\Omega_y} b(\mathrm{x})$, where Ω_y denotes the local region centered at pixel y. In practice, the degree of inhomogeneity is hardly stable due to illumination and device factors. That is, images with severe intensity inhomogeneity indicate that the variation degree is different at each local region with fixed size. Therefore, we define the term: variation degree of intensity inhomogeneity. In Fig. 1, two intensity inhomogeneities are separately shown in Fig. 1(b) and Fig. 1(f). Fig. 1(b) has the same variation degree in the whole image as shown in Fig. 1(d). However, the right of Fig. 1(f) has a greater variation degree than that of the left as shown in Fig. 1 (h).

Severe intensity inhomogeneity, as noted previously in [26, 29, 31], often causes problems in level set based segmentation. We define the intensity inhomogeneity b as a slowly varying function and the deviation of its first order is constant. On the contrary, severe inhomogeneity means that the variation degree of intensity inhomogeneity is not steady and varies in different local regions. In fact, severe intensity inhomogeneity is hardly defined by virtue of fixed features and can be divided into the following three types: First, the intensity inhomogeneity b is not uniform variation as shown in Fig. 2(a). Second, in the same object region as shown in Fig. 2(b), some local regions have larger intensity variation than that of other local regions. Third, as shown in Fig. 2(c), there are severe intensity overlaps between object and background regions, and the image is marred by a complicated background.

B. Brief Review of Three Representative Models

1) RSF Model

To improve the performance of the CV model, Li et al. [11, 12] proposed the RSF model by embedding the local information into a piecewise smooth model. The energy functional of the RSF model is written as follows:

$$E_{RSF} = \lambda_1 \iint_{in(c)} k_\sigma(\mathrm{x}-\mathrm{y}) \cdot \left(I(\mathrm{y}) - f_1(\mathrm{x})\right)^2 dy dx + \lambda_2 \iint_{out(c)} k_\sigma(\mathrm{x}-\mathrm{y}) \cdot (I(\mathrm{y}) - f_2(\mathrm{x}))^2 dy dx \quad (3)$$

where λ_1 and λ_2 are fixed parameters, I is an input image, and c denotes the evolution contour. f_1 and f_2 are the weighted intensity averages in a Gaussian window inside and outside c. k_σ is the Gaussian kernel with standard deviation σ, and μ and ν are two fixed parameters. The parameter σ is a constant to control the size of the local region. The local intensity information is introduced to enable the RSF model to handle intensity inhomogeneity problems. However, due to the variances of different local regions in the whole image, the intensity inhomogeneities cannot be described in local regions with fixed size for the whole image. Thus, the RSF model is generally unavailable for images with severe intensity inhomogeneity.

2) LIC Model

Li et al. [24] also proposed the LIC model, which incorporates the bias field estimation and a local intensity clustering criterion to address images with intensity inhomogeneities. The energy functional of the LIC model is written as follows:

$$E_{LIC} = \lambda_1 \iint_{in(c)} k_\sigma(\mathrm{x}-\mathrm{y}) \cdot \left(I(\mathrm{y}) - c_1 b(\mathrm{x})\right)^2 dy dx + \lambda_2 \iint_{out(c)} k_\sigma(\mathrm{x}-\mathrm{y}) \cdot (I(\mathrm{y}) - c_2 b(\mathrm{x}))^2 dy dx \quad (4)$$

where c_1 and c_2 are two constants to denote the intensity of two regions inside and outside of the contour, respectively. The term $b(\mathrm{x})$ approximates intensity inhomogeneities in the given image. According to the clustering criterion introduced in [24], the approximation of the clustering center of the local region can be defined as $c_1 b(\mathrm{x})$ or $c_2 b(\mathrm{x})$. The advantage of the LIC model is that it can segment some images with intensity inhomogeneity by using the cluster center to describe each pixel.

3) LSACM Model

In the LSACM model, the Gaussian distribution is used to model the intensity of object and background regions [31]. The means and variances of Gaussian distributions are mapped into the original image with a sliding window. The energy functional of the LSACM model is represented as follows:

$$E_{LSACM} = \sum_i \lambda_i \iint_{\Omega_i} k_{\sigma_i}(\mathrm{x}-\mathrm{y}) \cdot \left(\log(\sigma_i) + \frac{(I(\mathrm{y}) - b(\mathrm{x})c_i)^2}{2\sigma_i^2}\right) dy dx \quad (5)$$

where the energy functional is defined by the inverse log-likelihood function. σ_i is the standard deviation subject to the object in region Ω_i. LSACM can avoid the partial volume effect by averaging the neighboring pixel intensities in the same region. Meanwhile, LSACM is an extension of the LIC method.

III. METHODOLOGY

A. Problem Description

Constructing the desirable fitting function is a key factor for image segmentation. On the one hand, the optimal fitting function is utilized to discriminate object and background regions. On the other hand, the segmentation of local regional models is based on local approximation homogeneity. However, due to the nonlinear intensity distribution, the images with severe intensity inhomogeneity cannot satisfy this principle. Thus, the optimal fitting function can be utilized to improve the segmentation effects.

In this paper, we find that segmenting images with severe intensity inhomogeneities is essentially nonconvex due to the nonlinear distribution of the intensity variation of severe intensity inhomogeneity images. However, existing level set models such as [11-15, 24] utilize linear models to fit the nonlinear intensity distribution and hence may not be effective for the task. Consequently, nonlinear modeling is needed to address the issues.

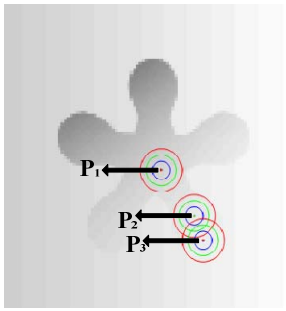

(a) Original image and nine circles with different center pixels and radii;

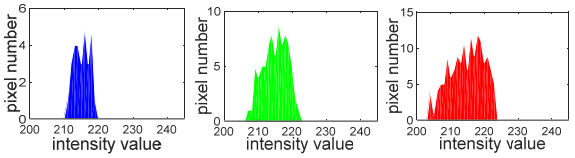

(b) the intensity histograms of three local regions centered at point P_1

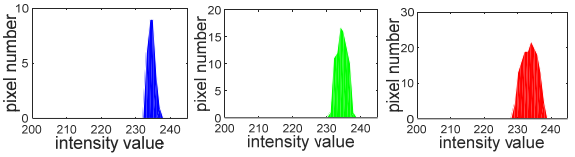

(c) the intensity histograms of three local regions centered at point P_2

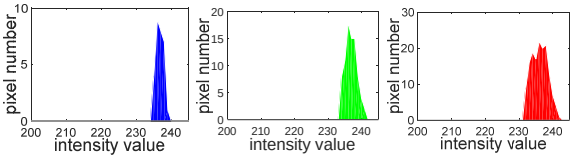

(d) the intensity histograms of three local regions centered at point P_3

Fig.3. The intensity distributions of local regions.

We give an example as shown in Fig. 3 to analyze the nonlinear distribution of intensity inhomogeneity. Fig. 3(a) shows an object with severe intensity inhomogeneity. In Fig. 3(a), the intensity contrast between object and background regions is gradually reduced from the top left to lower right. In the inside of the object, we set three points, *i.e.*,P_1, P_2 and P_3. Around each point, we draw three circles with different radii and different colors, *i.e.*, blue, green and red. The circles with the same color have the same radius. Fig. 1(b), (c), and (d) depict the intensity histograms of local regions enclosed by three circles centered at P_1, P_2 and P_3. Since the local regions centered at P_1 and P_2 are located in the inside of the object, we thought that the intensity distributions of local regions centered at P_1 and P_2 should be similar, and all local regions centered at P_1 and P_2 should not be divided. The other three local regions centered at P_3 include not only the object region but also the background region. That is, local regions centered at P_3 should be divided into two parts: object and background. From Fig. 3, two phenomena can be observed: (1) There is a significant difference between intensity distributions of local regions centered at P_1 and P_2, which indicates that the variation degrees of intensity inhomogeneity are different within the object. (2) The intensity distributions and the variation degrees of intensity inhomogeneity of local regions centered at P_2 and P_3 are almost the same, which illustrates that the traditional description term such as the intensity mean and variance cannot be used to discriminate the distributions of object and background regions for this image. That is, the local regions centered at P_3 are hardly divided according to the traditional description term.

B. Method Description

From Fig. 3, it can be seen that the intensity variation of the region interior may be higher than that of the edges, and the variation degrees of intensity inhomogeneities are different in each local region. That is, the intensity variation of the severe intensity inhomogeneity image is a nonlinear distribution. Thus, segmenting images with severe intensity inhomogeneity can be viewed as a nonconvex optimization problem. As described previously, a nonlinear description method is desirable to describe the fitting function and solve the associated nonconvex optimization problem, and Taylor expansion [32] is one of the classical nonlinear polynomial methods. The nonlinear polynomial method based on Taylor expansion is able to take more factors into account to improve the accuracy of the local region description. Considering the smoothness of local region of the image and the local effectiveness of Taylor expansion, we utilize the Taylor expansion to approximate the local region of the image and refer to the method as *Local Approximation of Taylor Expansion* (LATE). Consider a given vector valued image I: $\Omega \to \mathrm{R}$, where $\Omega \subset \mathrm{R}^n$ is the image domain. Let c be a closed contour in the image domain Ω, which separates Ω into two regions: $\Omega_1 = inside(c)$ and $\Omega_2 = outside(c)$. Based on the observations of smoothness in terms of pixel intensities among local regions, pixel intensity located at the local region is assumed to be a continuous and differentiable function. Accordingly, the relation between pixel intensity $I(\mathrm{x})$ and the corresponding pixel intensity $I(\mathrm{y})$ can be represented as follows:

$$I(\mathrm{x}) \approx I(\mathrm{y}) + I'(\mathrm{y})d + \cdots + \frac{I^{(n)}(\mathrm{y})}{n!}d^n \qquad \textbf{(6)}$$

where $\mathrm{y} \in \Omega_{\mathrm{x}}$ denotes the neighborhood centered at x. $d = \mathrm{x} - \mathrm{y}$ denotes a constant. We use R_i $(i \in \{1,2\})$ to denote the object and background regions. In addition, we then define a local intensity mean (*LIM*) to replace the term $I(\mathrm{y})$.

$$LIM_i(\mathrm{x}) = mean(I(\mathrm{y}): \mathrm{y} \in \Omega_{\mathrm{x}} \cap \mathrm{R}_i) \quad i \in \{1,2\} \qquad \textbf{(7)}$$

While the x is located in the object or background regions, the $I(\mathrm{y})$ can be separately denoted as follows:

$$I(\mathrm{y}) \approx \begin{cases} LIM_1(\mathrm{x}); & if\ \mathrm{x} \in \mathrm{R}_1 \\ LIM_2(\mathrm{x}); & if\ \mathrm{x} \in \mathrm{R}_2 \end{cases} \qquad \textbf{(8)}$$

In Eq.(6), the differential term $I'(\mathrm{y})d + \cdots + \frac{I^{(n)}(\mathrm{y})}{n!}d^n$ is regarded as the so-called adjusting term. To design a desirable adjusting term, we need to model and approach the differentials of Eq.(6). Considering the intensity inhomogeneity model as Eq.(5) shows, we transform the differential as follows:

$$I^{(q)}(\mathrm{y}) \approx b^{(q)}(\mathrm{y})C_i \qquad q \in [1, n] \qquad \textbf{(9)}$$

Meanwhile, the second-order differential $I''(\mathrm{y})$or higher order differentials $I^{(n)}(\mathrm{y})$may approach zero in the same region so that these differentials can be ignored in the proposed method. It should be noted that the first-order differential is denoted by the variation degree of intensity inhomogeneity.

Based on the above analysis and Eq.(6-9), Eq.(6) can be simplified as follows:

$$I(\mathrm{x}) \approx I(\mathrm{y}) + I'(\mathrm{y})d \qquad \textbf{(10)}$$

According to Eq.(8) and Eq.(9), Eq.(10) can be transformed as:

$$I(\mathrm{x}) \approx LIM_i(\mathrm{x}) + b'(\mathrm{y})C_i.d \quad \textbf{(11)}$$

Since both C_i and d are constants, the constant d of Eq.(11) can be ignored. Thus, we can get Eq.(12).

$$I(\mathrm{x}) \approx LIM_i(\mathrm{x}) + b'(\mathrm{y})C_i \quad \textbf{(12)}$$

where b' denotes the variation degree of intensity inhomogeneity. The images with severe intensity inhomogeneity have different variation degrees of intensity inhomogeneity. In Eq.(12), since the image intensity is described by the combination of local intensity statistics and the variation degree of intensity inhomogeneity, the proposed description Eq.(12) can better describe image intensity than other methods. According to the Taylor expansion approximation criterion, the local region in the same region can be accurately approximated. The above described local intensity approximation function indicates that the intensities of each region can be accurately described by the neighborhood pixels located in the same region based on the first-order Taylor expansion. This allows us to construct the energy functional, which is used to divide the image into the object or background regions. That is, each pixel can be approximated by the statistical intensity and differential information of the neighborhood. The energy functional is represented as follows:

$$\begin{aligned} E = &\int_{\Omega} \int_{in(c)} k_\sigma(\mathrm{x}-\mathrm{y})\,(I(\mathrm{x}) - LIM_1(\mathrm{x}) \\ &- b'(\mathrm{y})C_1)^2 dy d\mathrm{x} \\ +&\int_{\Omega} \int_{out(c)} k_\sigma(\mathrm{x}-\mathrm{y})\,(I(\mathrm{x}) - LIM_2(\mathrm{x}) \\ &- b'(\mathrm{y})C_2)^2 dy d\mathrm{x} \end{aligned} \quad \textbf{(13)}$$

where I denotes the original image, c denotes the evolving contour, $in(c)$ and $out(c)$ separately denote the inside and outside of the contour, and k_σ is the Gaussian kernel with standard deviation σ. The kernel function k decreases drastically to zero as y increases in distance from x. Specifically, only the intensities in the neighborhood are dominant in the energy functional. Thus, we use the kernel function k to control and obtain a local region around the point x. Then, the image segmentation is transformed as a minimization problem of the energy functional. While the approximation function $LIM_i(\mathrm{x}) + b'(\mathrm{y})C_i$ accurately approximates $I(\mathrm{x})$, the energy functional shall obtain the minimization value. Then, the image shall be accurately segmented.

The proposed LATE method solves the nonconvex optimization problem as mentioned before. Then, the optimal fitting is obtained and used to approximate the object and background regions. Specifically, according to the analysis in Section III-A, the local intensity distribution of a severe intensity inhomogeneity image is usually nonlinear. As a result, how to construct the effective fitting function and optimize the function are critical to such segmentation tasks. In traditional methods such as RSF and LIC, the optimization of the fitting function is treated as a nonconvex optimization problem. Here, to explain nonconvex optimization in detail, we take the RSF model as an example. Specifically, the energy functional of the RSF model is written as follows:

$$\begin{aligned} min\colon E_{RSF} = &\sum_{i=1}^{n} \iint_{\Omega_i} k_\sigma(x-y) \\ &\cdot (I(y) - f_i(x))^2 dy\, dx \end{aligned} \quad \textbf{(14)}$$

Since the premise is that the local region approximates intensity homogeneity, the energy functional has a constraint requesting the fitting function f_i to satisfy the condition:

$$f_i(\mathrm{x}+\Delta\mathrm{x}) - f_i(\mathrm{x}) = f_i(\mathrm{y}+\Delta\mathrm{x}) - f_i(\mathrm{y}) \quad \textbf{(15)}$$

where x and y denote the image pixel, and Δx denotes the pixel distance. Thus, $f_i{}'(\mathrm{x}) = constant$.

In reality, most local regions of real images cannot satisfy the constraint (Eq.(15)), making f_i a nonconvex set and the corresponding optimization nonconvex. Since Taylor expansion is a nonlinear high-order approximation method, we propose utilizing the Taylor expansion to approximate the fitting function and relax the constraint. Specifically, according to Eq.(12), the fitting function based on Taylor expansion is simplified as:

$$LIM_i(\mathrm{x}) + b'(\mathrm{y})C_i$$

The proposed energy functional is written as:

$$\begin{aligned} min\colon E_{LATE} = &\sum_{i=1}^{n} \iint_{\Omega_i} k_\sigma(\mathrm{x}-\mathrm{y}) \cdot (I(\mathrm{y}) - LIM_i(\mathrm{x}) \\ &- b'(\mathrm{y})C_i)^2 dy d\mathrm{x} \end{aligned} \quad \textbf{(16)}$$

That is, the constraint $f_i'(\mathrm{x}) = constant$ is cancelled. In the new energy functional, the first-order term $b'(\mathrm{y})$ is not required as a constant but regarded as a function that needs to be optimized. The $LIM_i(\mathrm{x})$ can be approximated by the local intensity mean. The intensity inhomogeneity $b(\mathrm{y})$ is set as: $b(\mathrm{y}) \in [0,2]$. Thus, the $LIM_i(\mathrm{x})$ and $b'(\mathrm{y})$ are separately defined as follows:

$$LIM_i(\mathrm{x}) = \{LIM_i\colon \Omega \to [0,255] |\ \forall \mathrm{x} \in \Omega\}$$
$$b'(\mathrm{y}) = \{b'\colon \Omega \to [0,2] |\ \forall \mathrm{y} \in \Omega_{\mathrm{x}}\}$$

Here, $LIM_i(\mathrm{x})$ and $b'(\mathrm{y})$ are two continuous and convex sets. Therefore, by relaxing the constraint, the single nonconvex optimization problem ($f_i(\mathrm{x})$) has been revised as two convex optimizations ($LIM_i(\mathrm{x})$ and $b'(\mathrm{y})$).

In addition, it is necessary to elaborate on the meaning of the approximation function. Based on the first-order Taylor expansion, the fidelity term and adjusting term are joined to construct the proposed approximation function. The approximation function including intensity and differential information is a nonlinear representation of the image intensity outside and inside of the contour. The fidelity term describes the intensity of the original image by virtue of the statistics for local intensity information. The adjusting term represented by the variation degree of intensity inhomogeneity is used to adjust the approximation bias of each local region. Meanwhile, the first-order differential is very small in smooth local regions located in the same region. However, while the local regions include image edges, the first-order differential of local regions would be a bigger value. That is, the local contrast of an image can be enhanced by the proposed LATE method. Meanwhile, in the approximation method based on Taylor expansion, while the neighborhood pixel y and x are located in the same region, the approximation difference is very small and vice versa.

In Fig. 4, we present an example to testify to the

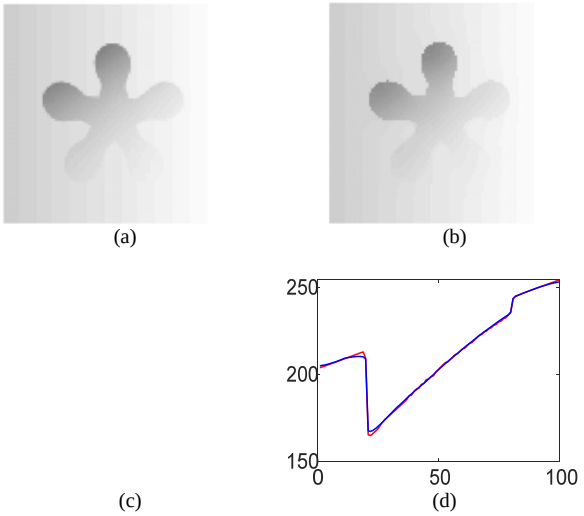

Fig. 4. The approximation degree of the proposed method. (a) Original image; (b) approximated image; (c) the histograms of the original image and approximated image; (d) cross-section of middle rows of original image (red curve) and approximated image (blue curve).

approximation precision of the proposed approximation function. The object region of the original image shown in Fig. 4(a) has a very big intensity difference. The approximated image shown in Fig. 4(b) is derived by utilizing the proposed approximation method. The intensity histograms of the original and approximated images are also very similar as shown in Fig. 4(c). In Fig. 4(d), we show the intensity approximation curves of the middle row of the image to further demonstrate the precision of the proposed approximation. It can be seen that the difference between the approximated image and original image is very small.

Next, we shall show that the proposed method can improve the approximation degree and enhance the contrast of images. First, a representation formulation of contrast is given. The contrast is defined and denoted by the formulation, which is the ratio of energy change caused by contour evolution to the previous energy value.

$$R_C = \frac{|E_{n+1} - E_n|}{E_n} \tag{17}$$

where E_n and E_{n+1} denote the energy values of n^{th} iteration and $(n+1)^{\text{th}}$ iteration, respectively. The ratio R_C reflects the statistical change information of the local region. If R_C is bigger, the contrast in the local region statistical information is bigger, so that the discrimination of the local region is higher, and vice versa.

In Fig. 5, we provide a comparison experiment to show the efficiency of the proposed method. The proposed LATE method is based on the first-order Taylor expansion, which is represented by the variation degree of intensity inhomogeneity and called the adjusting term. The compared method is referred to as Local Approximation (LA), which is a variant of the LATE method canceling the variation degree of intensity inhomogeneity. By comparing LA and LATE methods, we shall derive the advantages of the proposed adjusting term. Specifically, the contour evolving process is shown in Fig. 5(a). The vertical ordinates of Fig. 5(b) and (c) denote iteration times. The energy values and energy variance degrees are shown in Fig. 5(b) and (c), respectively. It should be noted in Fig. 5(b) that both energy values of LATE and LA are decreased with the contour evolving. Meanwhile, the energy values of LATE are still smaller than that of LA at each iteration. However, the energy variation degree is bigger than that of the LA method as shown in Fig. 5(c), which means that the contrast is enhanced by the LATE method. Therefore, the adjusting term, which enhances the contrast of the local region, plays an important role in the segmentation process.

In a word, the proposed LATE method can improve the approximation precision and enhance the local contrast of the image. Hence, the LATE method can achieve desirable segmentation results for those images with severe intensity inhomogeneity.

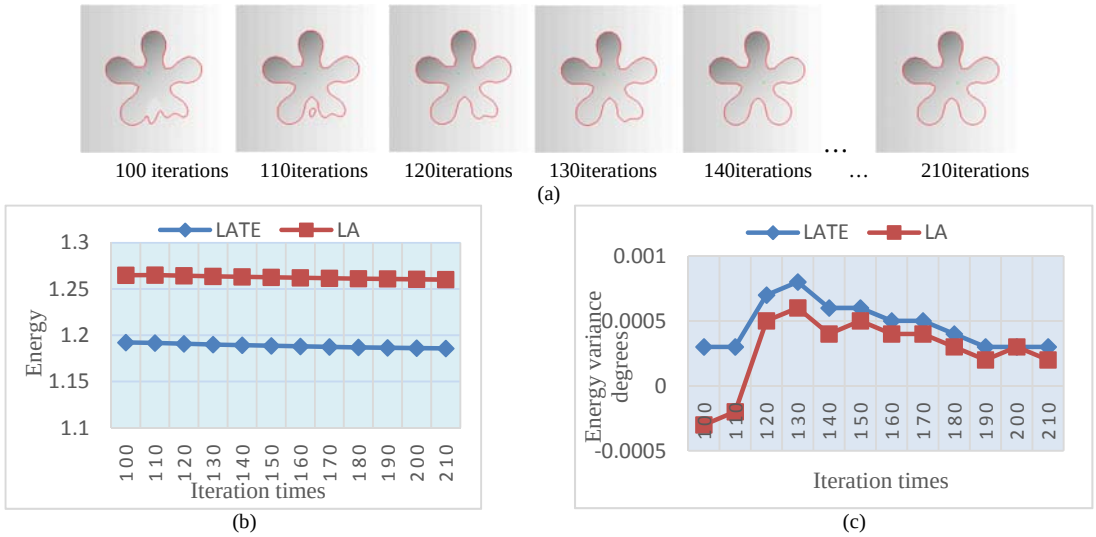

Fig. 5. The analyzation of approximation degree and contrast: (a) the evolving process of contour; (b) the energy variances of LA and LATE in evolving process; (c) the variance degrees of LA and LATE of each ten iterations.

C. Discussions

In this section, we will explain the advantages of the LATE method over other existing methods. In the proposed LATE method, it is the first time that the first-order Taylor expansion is introduced to effectively approximate the intensity inhomogeneity images. Unlike existing methods, LATE uses the statistical intensity information of the neighborhood as a fidelity term and the first-order differential as the adjusting term. The local intensity mean as the statistic information is used to approximate the local region and ensure the approximation effectiveness. The adjusting term implies variation degrees of intensity inhomogeneity and includes edge information (differential information). It can be used to adjust the approximation description bias, which gives the approximation strong specificity. It should be noted that the fidelity and adjusting terms in LATE are not independent but jointly used to approximate image intensity. In the LATE model, both the region statistical information and variation degree of intensity inhomogeneity are jointly used to ensure the precision of approximation and enhance the image contrast. Thus, the local approximation of our method is more accurate and robust.

The proposed LATE method can be regarded as the constraint relaxation of several classical methods such as RSF and LIC models. However, the applicability and robustness of the LATE model is better than that of the classical methods. The local region-based models have already been used to segment intensity inhomogeneity images. Both the RSF model [11] and LIC model [24] are successful examples. However, we highlight that the proposed method relaxes the constraint of these local region-based models. Here, we testify that LATE realizes constraint relaxation for the RSF and LIC models in theory.

Compared with RSF: The approximation function of the proposed LATE method and RSF model are separately denoted by $LIM_i(\mathrm{x}) + b'(\mathrm{y})C_i$ and $f_i(\mathrm{y})$. According to Eq.(8), $LIM_i(\mathrm{x}) \approx I(\mathrm{y})$. C_i is constant, and $LIM_i(\mathrm{x}) + b'(\mathrm{y})C_i$ can be denoted by the function on y:

$$LIM_i(\mathrm{x}) + b'(\mathrm{y})C_i \approx I(\mathrm{y}) + b'(\mathrm{y})C_i \tag{18}$$

That is, both $I(\mathrm{y}) + b'(\mathrm{y})C_i$ and $f_i(\mathrm{y})$ can be seen as a function with independent variables 'y' and 'i'. Thus, the LATE can be regarded as the extended formulation of RSF. Therefore, by reformulating the representation as Eq.(13), the RSF model is a special case of LATE.

Compared with LIC: We transform the approximation function of the LATE method. Then, the formulation can be replaced by the following formulation:

$$\begin{aligned} LIM_i(\mathrm{x}) + b'(\mathrm{y})C_i &\approx I(\mathrm{y}) + b'(\mathrm{y})C_i \\ &\approx b(\mathrm{y})C_i + b'(\mathrm{y})C_i \\ &= \big(b(\mathrm{y}) + b'(\mathrm{y})\big)C_i \end{aligned} \tag{19}$$

Both the formulation $b(\mathrm{y}) + b'(\mathrm{y})$ and $b(\mathrm{y})$ can be regarded as the function with independent variable 'y'. Therefore, LATE is also the extended formulation of the LIC model.

Eq.(18) and Eq.(19) show that LATE is the relaxation formulation of the RSF and LIC models. That is, the segmentation ability of LATE is at least the same or better than the RSF and LIC models. Hence, the applicability and robustness of LATE is stronger than other existing methods. Meanwhile, the proposed LATE method can also be extended to the energy functional based on Gaussian distribution as follows.

$$E = \sum_{i=1}^{2} \iint_{\Omega_i} \frac{1}{\sqrt{2\pi}\sigma_i} \exp\left(-\frac{(I(\mathrm{x}) - LIM_i(\mathrm{x}) - b'(\mathrm{y})C_i)^2}{\sigma_i^2}\right) d\mathrm{x}d\mathrm{y} \tag{20}$$

The meaning of the energy functional based on a Gaussian distribution is explained as follows: In general, it can be assumed that the intensity values of different regions on the same object can be modeled as a finite Gaussian distribution. Under this assumption, all pixels belonging to the same distribution should be divided into the same region. In Eq.(20), the $LIM_i(\mathrm{x}) + b'(\mathrm{y})C_i$ is regarded as a local intensity center. It is noted that each local region has a special local intensity center that is also adjusted by the variation degree of intensity inhomogeneity $b'(\mathrm{y})C_i$. σ_i is the variance of the i^{th} region.

D. Level Set Formulation

Since energy minimization can be solved by using the curve implicitly combined with a level set function ϕ, we use the level set method to obtain final segmentation results. In the level set method, the evolving contour c is represented by the zero level set of a Lipschitz function:ϕ: $\Omega \rightarrow$ R. By using the Heaviside function H, the energy functional Eq.(14) can be expressed as follows:

$$\begin{aligned} E = \iint_{\Omega} k_\sigma(\mathrm{x}-\mathrm{y})(I(\mathrm{x}) - LIM_1(\mathrm{x}) - b'(\mathrm{y})C_1)^2 \cdot H(\phi) d\mathrm{y}d\mathrm{x} \\ + \iint_{\Omega} k_\sigma(\mathrm{x}-\mathrm{y})(I(\mathrm{x}) - LIM_2(\mathrm{x}) - b'(\mathrm{y})C_2)^2 \cdot (1 - H(\phi)) d\mathrm{y}d\mathrm{x} \end{aligned} \tag{21}$$

Here, H is approximated by the following formula:

$$H(\mathrm{x}) = \frac{1}{2}\left[1 + \frac{2}{\pi} \cdot \arctan\left(\frac{\mathrm{x}}{\varepsilon}\right)\right] \tag{22}$$

The differential of H is written as:

$$\delta(\mathrm{x}) = H'(\mathrm{x}) = \frac{1}{\pi}\frac{\varepsilon}{\varepsilon^2 + \mathrm{x}^2} \tag{23}$$

Then, we use the standard gradient descent method to minimize Eq.(21). C_1, C_2 and $b'(\mathrm{y})$ are derived by minimizing Eq.(21). First, for fixed ϕ and $b'(\mathrm{y})$ (we initialize ϕ and $b'(\mathrm{y})$ according to the strategy introduced in the next section), the two constants C_1 and C_2 can be obtained by minimizing energy E_D:

$$C_1 = \frac{\iint_{\Omega} k_\sigma(\mathrm{x}-\mathrm{y}) \cdot (I(\mathrm{x}) - LIM_1(\mathrm{x})) \cdot H(\phi) d\mathrm{y}d\mathrm{x}}{\iint_{\Omega} k_\sigma(\mathrm{x}-\mathrm{y}) \cdot b'(\mathrm{y}) H(\phi) d\mathrm{y}d\mathrm{x}} \tag{24}$$

$$C_2 = \frac{\iint_{\Omega} k_\sigma(\mathrm{x}-\mathrm{y}) \cdot (I(\mathrm{x}) - LIM_2(\mathrm{x})) \cdot (1 - H(\phi)) d\mathrm{y}d\mathrm{x}}{\iint_{\Omega} k_\sigma(\mathrm{x}-\mathrm{y}) \cdot b'(\mathrm{y})(1 - H(\phi)) d\mathrm{y}d\mathrm{x}} \tag{25}$$

For fixed C_1, C_2 and ϕ, the optimal $b'(\mathrm{y})$ can be derived by minimizing the data term E_D. Thus, we can obtain Eq.(26).

To regularize the level set function, two regularization terms proposed in [12] are introduced. Finally, the total energy functional of our model can be written as Eq.(27):

$$E = \iint_{\Omega} k_\sigma(\mathrm{x}-\mathrm{y})(I(\mathrm{x}) - LIM_1(\mathrm{x}) - b'(\mathrm{y})C_1)^2 \cdot H(\phi)d\mathrm{y}d\mathrm{x} + \iint_{\Omega} k_\sigma(\mathrm{x}-\mathrm{y})(I(\mathrm{x}) - LIM_2(\mathrm{x}) - b'(\mathrm{y})C_2)^2 \cdot \big(1 - H(\phi)\big)d\mathrm{y}d\mathrm{x} + \mu\int_{\Omega} |\nabla H(\phi)|d\mathrm{x} + v\int_{\Omega} (|\nabla\phi| - 1)^2 d\mathrm{x} \quad (27)$$

where v and μ are two constant parameters. v is a constant weight of curve length term $\int_{\Omega} |\nabla H(\phi)|d\mathrm{x}$, which is used to smooth the evolution contour. μ is a constant weight of regularization term $\int_{\Omega} (|\nabla\phi| - 1)^2 d\mathrm{x}$, which is used to keep the level set as a signal distance function to avoid reinitialization of the curve. σ ($\sigma = 4r + 1$) is the scale parameter of Gaussian kernel function k_σ. r is constant, which is used to control the local region size.

By minimizing the energy functional in Eq.(27), we can obtain the optimal image segmentation results. The solution to the energy minimization with respect to ϕ by the gradient descendent method can be obtained.

For fixed C_1, C_2 and $b'(\mathrm{y})$, the minimization of $\mathrm{E}(\phi, C_1, C_2, b')$ with respect to ϕ can be achieved by using the standard gradient descent method:

$$\frac{\partial\phi}{\partial t} = -\frac{\partial E}{\partial\phi} \quad (28)$$

Then, the corresponding gradient flow equation can be written as Eq.(29). In Eq.(29), ∇ is the gradient operator, and $\mathrm{div}(\cdot)$ is the divergence operator.

E. Multiphase LATE

The proposed LATE method can also be extended to segment images with multiple objects. One level set function ϕ can only represent two regions: inside and outside the contour.

$$M_1(\phi) = H(\phi_1)$$
$$M_2(\phi) = (1 - H(\phi_1)) \quad (30)$$

This is referred to as two-phase indicators, which can be used to segment a single object. For the case of the multiphase, we can use two or more level set functions to define membership functions of the regions ϕ_1, ϕ_2. For example, if there exist four different regions, two level set functions, *i.e.*, ϕ_1, ϕ_2, can be used to represent all four different regions such that any two adjacent regions can be indicated by different colors. This is called the four-phase model. Here, we define the phase indicators as follows.

$$M_1(\phi) = H(\phi_1)H(\phi_2)$$
$$M_2(\phi) = (1 - H(\phi_1))H(\phi_2)$$
$$M_3(\phi) = H(\phi_1)(1 - H(\phi_2))$$
$$M_4(\phi) = (1 - H(\phi_1))(1 - H(\phi_2)) \quad (31)$$

Specifically, the four-phase model can be denoted by the following format:

$$E = \sum_{i=1}^{4}\left\{\iint_{\Omega} k_\sigma(\mathrm{x}-\mathrm{y})\big(I(\mathrm{x}) - LIM_i(\mathrm{x}) - b'(\mathrm{y})C_i\big)^2 \cdot M_i(\phi)d\mathrm{y}d\mathrm{x}\right\} + \sum_{p=1}^{2}\left\{\mu\int_{\Omega} |\nabla H(\phi_p)|d\mathrm{x} + v\int_{\Omega} \big(|\nabla\phi_p| - 1\big)^2 d\mathrm{x}\right\} \quad (32)$$

where i denotes the number of object regions. p denotes the number of ϕ.

F. Algorithm Summary

Here, we summarize the proposed LATE method by the following steps:

Step1: Input image I and parameters $v = 1$ and μ

Step2: Initialize ϕ^0 and set b' as a nonzero constant matrix, iteration times m, $\sigma = 4r + 1$

Step3: Compute C_1, C_2 using Eq. (24) and Eq. (25) with ϕ^j and b'

Step4: Compute b' using Eq. (26) with ϕ^j and C_1, C_2

Step5: Compute ϕ^{j+1} using Eq. (29) until the fixed iteration times $j + 1 = m$. Or else, return to step3.

IV. EXPERIMENTAL RESULTS

The proposed LATE method is tested on synthetic and real images from different modalities. The parameter μ of the proposed LATE method is selected from three values: 0.0001 $\times 255^2$, 0.001×255^2, and 0.01×255^2 for all experiments in this paper. The scale parameter r is discussed in Section IV-D in detail. The proposed method was implemented by MATLAB 2015 on a computer with Intel Core i7-3770, 3.4 GHz CPU, 8G RAM, and Windows 10 operating system.

A. Experimental Results on Four Synthetic Images

Fig. 6 shows the segmentation results of the LATE method for four synthetic images, in which four different intensity features are separately presented. In the first image, the intensity overlaps between object and background regions are obvious. The second image suffers from non-uniform

$$b'(\mathbf{y}) = \frac{\int_{\Omega} k_\sigma(\mathrm{x}-\mathrm{y})((I(\mathrm{x}) - LIM_1(\mathrm{x}))\cdot C_1\cdot H(\phi) + (I(\mathrm{x}) - LIM_2(\mathrm{x}))\cdot C_2\cdot(1 - H(\phi)))d\mathrm{x}}{\int_{\Omega} k_\sigma(\mathrm{x}-\mathrm{y})(C_1^2\cdot H(\phi) + C_2^2\cdot(1 - H(\phi)))d\mathrm{x}} \quad (26)$$

$$\frac{\partial\phi}{\partial t} = -\delta(\phi)(\int_{\Omega} k_\sigma(\mathrm{x}-\mathrm{y})(I(\mathrm{x}) - LIM_1(\mathrm{x}) - b'(\mathrm{y})C_1)^2 d\mathrm{y} - \int_{\Omega} k_\sigma(\mathrm{x}-\mathrm{y})(I(\mathrm{x}) - LIM_2(\mathrm{x}) - b'(\mathrm{y})C_2)^2 d\mathrm{y} + \mu\delta(\phi)\cdot div\left(\frac{\nabla\phi}{|\nabla\phi|}\right) + v(\nabla^2\phi - div\left(\frac{\nabla\phi}{|\nabla\phi|}\right)) \quad (29)$$

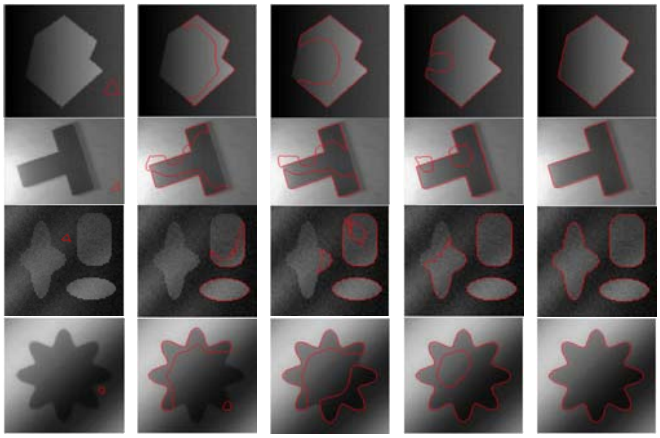

(a) (b) (c) (d) (e)

Fig. 6. Segmentation process and results of LATE method.

illumination. In the third image, three objects separately suffer from different variation degrees of intensity inhomogeneity. In the last image, severe intensity inhomogeneity is imposed. The curve evolution processes are depicted by showing the initial contours (Fig. 6(a)), intermediate contours (Fig. 6(b-d)), and final contours (Fig. 6(e)) on the images. Obviously, the experimental results show that the proposed LATE can achieve desirable segmentation results for all images with different intensity inhomogeneities.

B. Comparison Experiments

We conduct a series of comparison experiments to show the superiority of the LATE method. Several representative level set methods are selected for a performance comparison including the RSF model [12], LCV model [20], LIC model [24], and LSACM model [31]. All methods are exploited to segment three types of images including synthetic images, medical images and natural images. Among these experiments, segmentation on the synthetic image is used to elaborate that the LATE method can better segment images with severe intensity inhomogeneity than other models. The experiments for segmenting medical images and natural images are used to show the applicability and robustness of the LATE method. Most importantly, real image segmentation can be further used to illustrate the advantages and meaning of the proposed method.

1) Segmentation results on synthetic images

In this experiment, to obtain the best results, we still predefine optimal parameters including local region scales and initial contours for all four compared models [12, 20, 24, 31]. The segmentation results of the four comparison models are denoted by blue contours and separately shown in Fig. 7(a-d). The final segmentation results of the LATE method are denoted by red contours as shown in Fig. 7(e). Obviously, the four compared models often obtain failed segmentation results, while LATE successfully segmented these images. To obtain the ground truths, we first invite six individuals to delineate the object boundary Then, we obtain six binary masks (for example, intensity values of the object region are set as 1 and the background region is 0). Then, we analyze six masks to obtain a final desirable mask. Specifically, while the pixel is approved as the object pixel by at least four individuals, the pixel shall be regarded as the object pixel. Otherwise, the pixel shall be regarded as a background pixel. Then, to further measure the quality of the extracted objects, we utilize the Jaccard similarity coefficient (JSC) as a quantitative measure to evaluate the segmentation results of five methods.

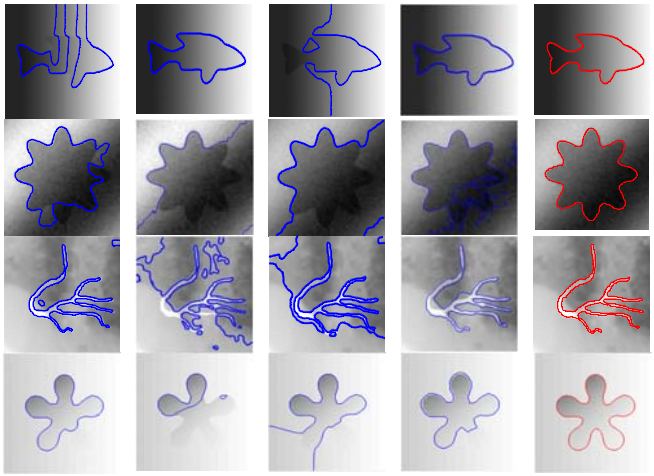

(a) (b) (c) (d) (e)

Fig. 7. The comparison experiments of the four models and LATE for segmenting synthetic images: (a) RSF; (b) LCV; (c) LIC; (d) LSACM; (e) LATE.

Table I. JSC OBTAINED BY THE RSF, LCV, LIC AND LSACM MODEL AND THE PROPOSED METHOD FOR FOUR IMAGES IN FIG.7

Method	Row1	Row2	Row3	Row4
RSF	0.8879	0.7796	0.8531	0.8757
LCV	0.9945	0.5037	0.5327	0.6323
LIC	0.5424	0.5887	0.6696	0.8028
LSACM	0.9951	0.8637	0.8290	0.8839
LATE	**0.9967**	**0.9918**	**0.9987**	**0.9983**

$$JSC(O_m, O_t) = \frac{A(O_m \cap O_t)}{A(O_m \cup O_t)} \quad \textbf{(33)}$$

where O_m denotes the derived object region by the algorithm and O_t denotes the corresponding object region in the ground truth image. A(·) represents the area of the region. It is noted that the JSC is bounded in [0, 1], and a larger value implies a more accurate segmentation.

The corresponding JSC values of the five methods for Fig. 7 are shown in Table I. It can be seen that the LATE method is superior in terms of accuracy to the other four models. Due to the local variations of intensity inhomogeneity, these models [12,20,24,31] cannot accurately describe all the local regions with fixed scales for all pixel points. Therefore, they often failed to segment the images in Fig. 7. The LATE method improves the approximation degree and enhances local contrast by presenting the approximation based on Taylor expansion. Thus, desirable segmentation results are obtained by the LATE method.

2) Segmentation results on medical images

Medical images have already been widely used to diagnose diseases. However, due to the influences of devices or illumination, there often exist intensity inhomogeneities in

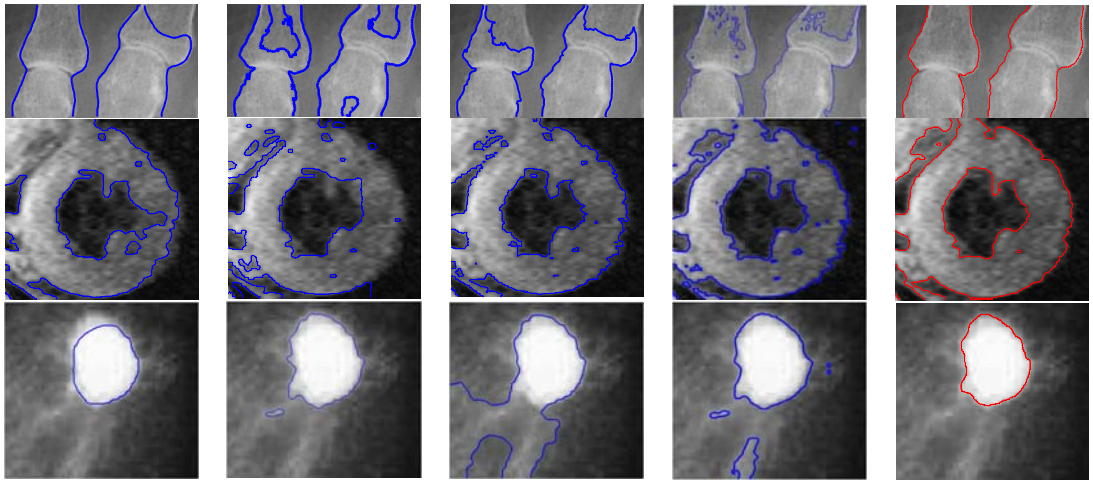

(a) (b) (c) (d) (e)

Fig. 8. Comparison experiments between four models and LATE for segmenting medical images: (a) RSF; (b) LCV; (c) LIC; (d) LSACM; (e) LATE.

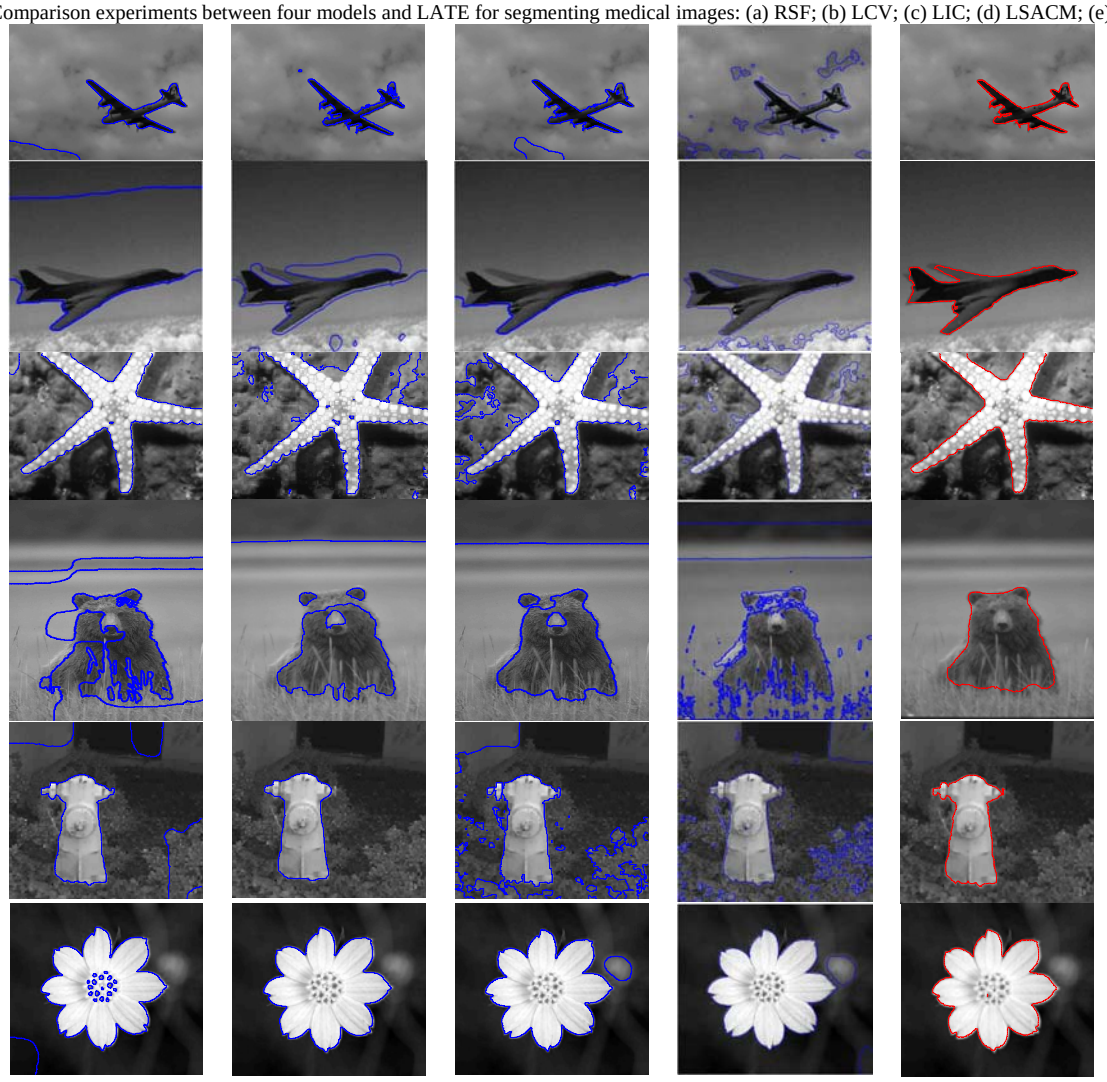

(a) (b) (c) (d) (e)

Fig. 9. Comparison experiments between four models and LATE for segmenting natural images: (a) RSF; (b) LCV; (c) LIC; (d) LSACM; (e) LATE.

medical images. In Fig. 8, the three medical images are an X-ray bone image, ventricular image and tumor image. These three types of images often suffer from intensity inhomogeneity. Here, the three medical images in Fig. 8 are segmented to demonstrate the superiority of the proposed method for medical image segmentation.

The segmentation results of the RSF, LCV, LIC and LSACM models are separately shown in Fig. 8(a-d). For the bone image,

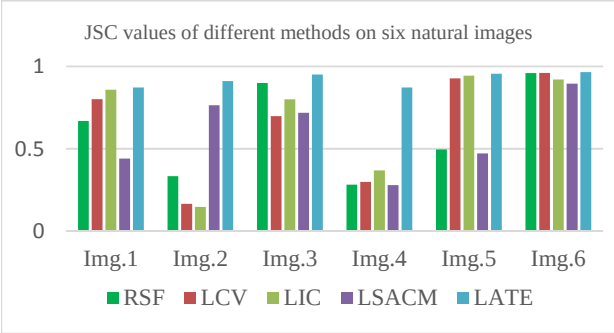

Fig. 10. JSC values of different methods on six natural images shown in Fig.9.

all four models cannot detect the weak boundary region so that they fail to segment this image. Both object and background regions of the heart image suffer from intensity inhomogeneity. Over-segmentation or under-segmentation have also emerged in these four models. However, the LATE method can still accurately segment all images (the red contours shown in Fig. 8(e)). In the last image of Fig. 8, LATE can derive a smoother object boundary than that of the other four models.

3) Segmentation results on natural images

In Fig. 9, we conduct more experiments on six natural images to evaluate the performances of the proposed LATE method. Six natural images suffer different intensity inhomogeneities including object region inhomogeneity (Row1 and Row6), background region inhomogeneity (Row 2 and Row 4), and complicated background obstacles (Row3 and Row5). It can be seen that the complicated backgrounds are emerged in these images. Meanwhile, the objects of the images are disturbed by intensity inhomogeneity. The segmentation of the RSF, LCV, LIC and LSACM models (as shown in Fig. 9(a-d)) has often failed. LATE can segment the six natural images accurately. The JSC values of the five models are shown in Fig. 10. Obviously, the accuracy of the proposed LATE model is higher than the other models.

In practice, the natural images are very complicated and various. To further demonstrate the segmentation capability of the proposed method for intensity inhomogeneous images, we add an experiment in which twenty images, mainly from the datasets Weizmann [35] and BSD500 [36], are segmented by the proposed LATE method as shown in Fig. 11. Since the proposed LATE method is applied to segment intensity homogeneous images, all twenty of the natural images have classical intensity inhomogeneous features. Therefore, the experiment is utilized to demonstrate the process capacity of the LATE for intensity inhomogeneity.

4) Segmentation results on multiphase objects

The results of multiphase segmentation are shown in Fig. 12. In Fig. 12, the first image to be segmented is an intensity inhomogeneous image with two objects. The second image to be segmented is contaminated by noise and contains three objects. The last two magnetic resonance (MR) images to be segmented are made up of gray matter, white matter and cerebrospinal fluid. From Fig. 12, it can be seen that the multiphase LATE method can accurately segment these images, which shows the ability to segment multiple objects.

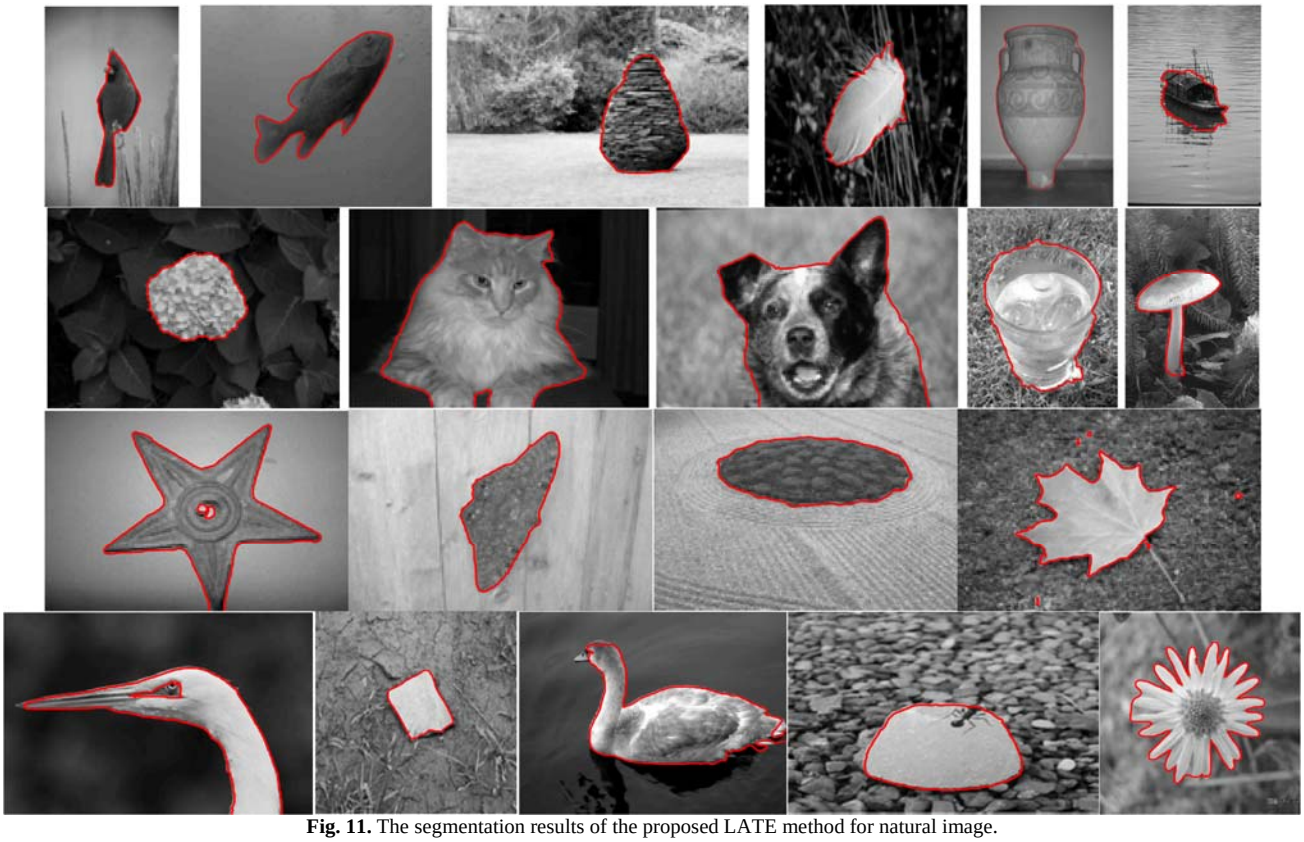

Fig. 11. The segmentation results of the proposed LATE method for natural image.

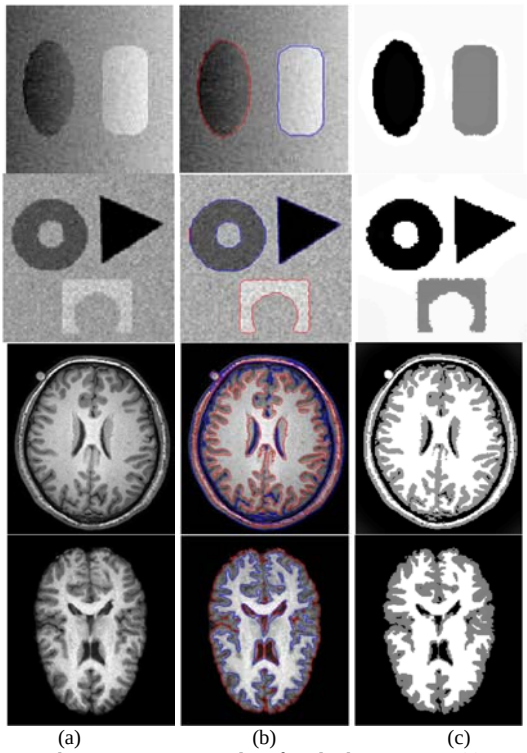

(a) (b) (c)

Fig. 12. The segmentation results of multiphase LATE: (a): original images; (b) final results based on color contours; (c) segmentation results.

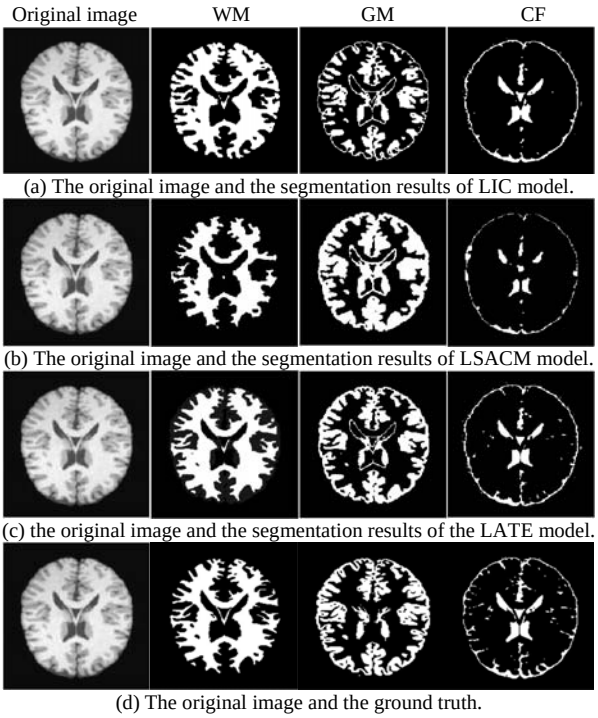

(a) The original image and the segmentation results of LIC model.

(b) The original image and the segmentation results of LSACM model.

(c) the original image and the segmentation results of the LATE model.

(d) The original image and the ground truth.

Fig. 13. Segmentation comparison between the LIC model, LSACM model and the proposed LATE method.

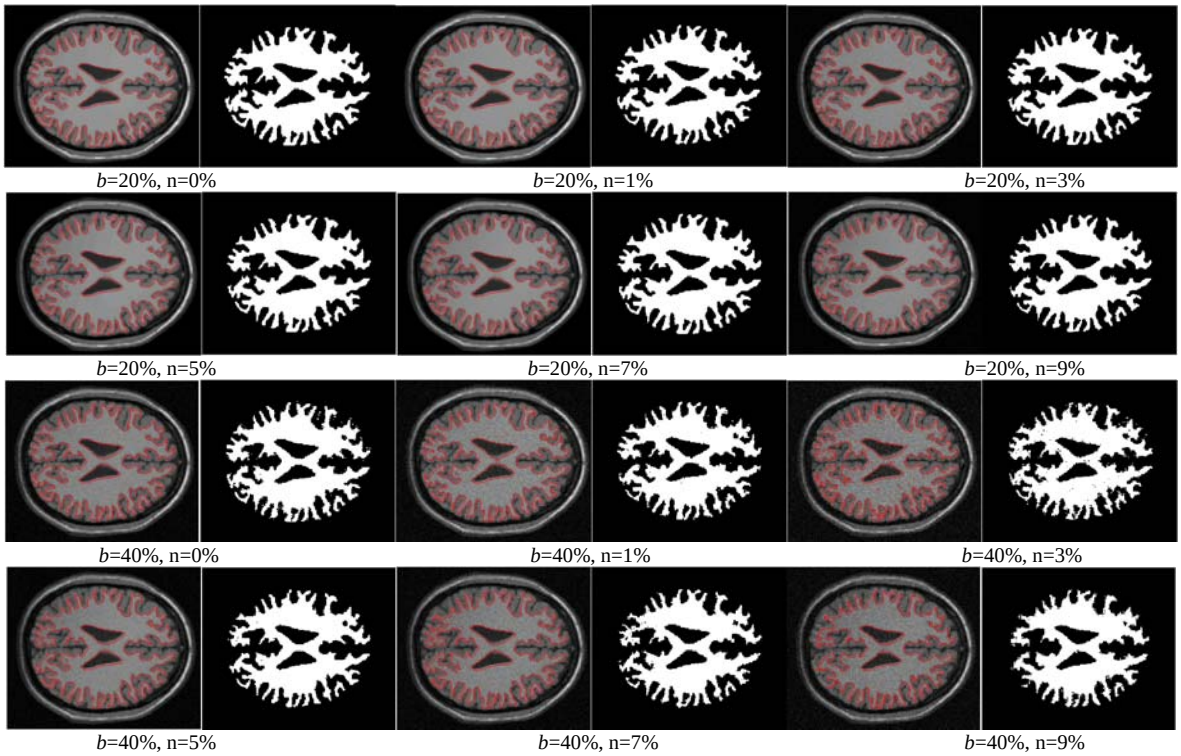

Fig. 14. The segmentation results of the LATE method for different intensity inhomogeneities and noise levels.

In the area of medicine, many research applications using MR images involve segmenting images with intensity inhomogeneity. Hence, to further demonstrate the superiority of the LATE model, we add a comparison experiment on the MRI brain image segmentation. This dataset is from http://www.bic.mni.mcgill.ca/brainweb/, and we choose a noise level of 7% and non-uniformity (“RF”) of 20%. There are three classes that should be segmented: cerebrospinal fluid

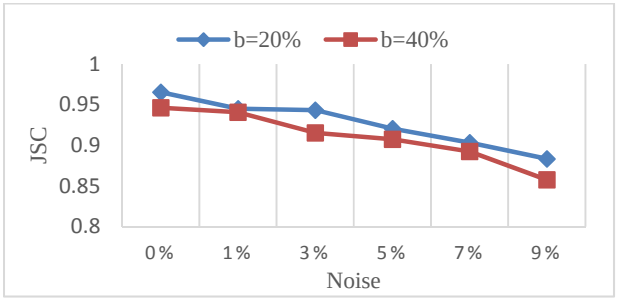

Fig. 15. Robustness of the proposed LATE method for different intensity inhomogeneities and noises.

(CF), gray matter (GM) and white matter (WM). Fig. 13 provides the segmented results of the LIC model, the LSACM model, the LATE model and the ground truth. We find that our proposed LATE model can produce much better results than the other two models.

C. Robustness Analysis

It is important that an automated segmentation procedure be robust with respect to different intensity bias statuses, noise levels, and initial contours. In this subsection, we further evaluate the performance of the LATE method on these aspects.

1) Robustness analysis for different intensity inhomogeneities and noises

We conduct experiments on magnetic resonance (MR) images to test the capability of the proposed LATE method for different intensity inhomogeneities and noise levels. The results are shown in Fig. 14. The original MR images are obtained from BrainWeb [33]. We use 'b' and 'n' to denote intensity inhomogeneity and noise, respectively. The different intensity inhomogeneities (b=20%, b=40%) and noise levels (n=0%, n=1%, n=3%, n=5%, n=7%, n=9%) are added to the MR images. The JSCs of the segmentation results are presented in Fig. 15. From the results shown in Fig. 15, we can see that the proposed method consistently returns reasonable partitions of the image, and accuracy can be slightly affected by the noise level.

In addition, to further demonstrate the superiority of LATE, we compare the LSACM [31] and Multiplicative Intrinsic Component Optimization (MICO) [34] by segmenting MRI images with different intensity inhomogeneities. In Fig. 16, the intensity inhomogeneities of the original images are gradually highlighted from left to right as shown in Fig. 16 (a), and the segmentation results of LSACM, MICO and LATE are presented in Fig. 16(b), (c) and (d), respectively. It can be seen that the LATE method can achieve better segmentation details than the other two methods.

2) Robustness analysis for initialization

Due to the introduction of first order Taylor expansion, the local intensity distribution is accurately approximated in the process of contour evolution. Here, we quantitatively evaluate the performance of the LATE method with different initial contours. The different initial contours (red contours shown in Fig. 17(a)) and the corresponding JSC values (as shown in Fig. 17(b)) of the segmentation results of the LATE method are shown in Fig. 17. Despite the great difference among these

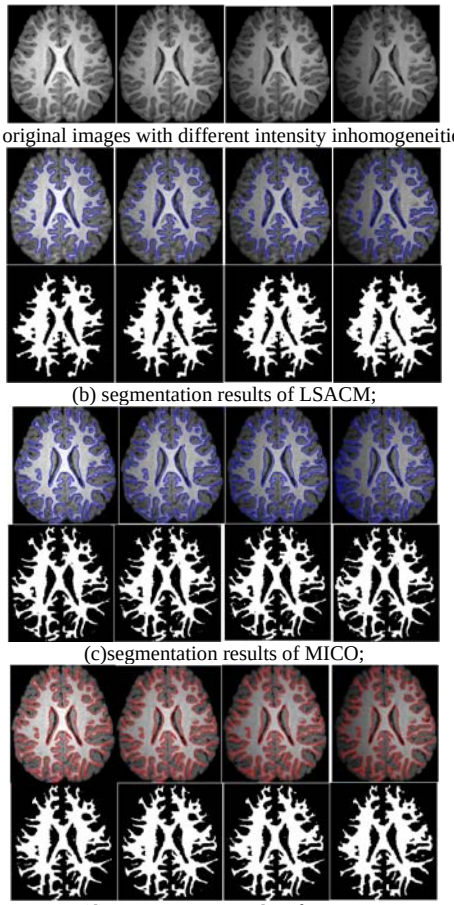

(a) original images with different intensity inhomogeneities;

(b) segmentation results of LSACM;

(c)segmentation results of MICO;

(d) segmentation results of LATE;

Fig. 16. The comparison between LSACM, MICO and the proposed LATE method for MRI images with different intensity inhomogeneities

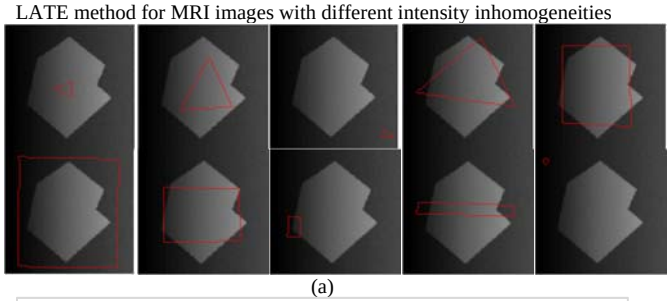

(a)

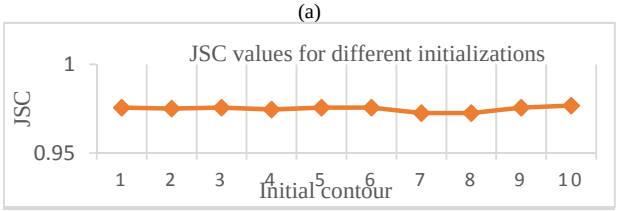

(b)

Fig. 17. Segmentation accuracy of LATE for 10 different initializations: (a) 10 different initial contours; (b) the JSC values of 10 segmentation results of LATE.

initial contours, the corresponding segmentation results of the LATE method are all capable of accurately capturing the object boundaries, which are almost the same.

In addition, the LATE method can accurately segment images by using a plane for initialization. That is, we can accurately segment images without an initial contour by using the LATE method. In Fig. 18, all four intensity inhomogeneity images without initial contours are accurately segmented using

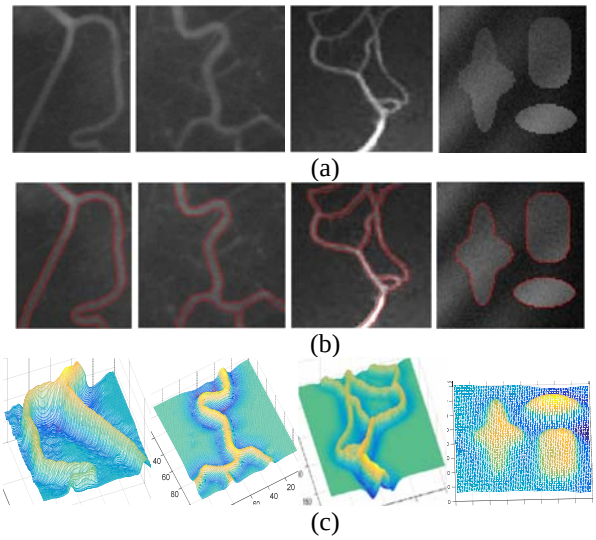

Fig. 18. Segmentation results of the LATE method without initialization contours. (a) original images; (b) segmentation results; (c) final level sets.

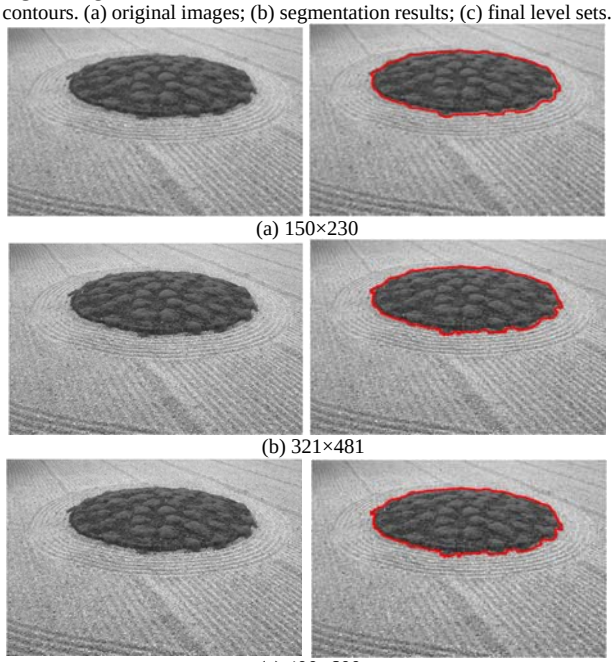

Fig. 19. Segmentation results of images with different resolution ratios.

the LATE method as shown in Fig. 18(b). The initial level sets are fixed as a plane so that the initial contours do not exist. The final level sets are smooth and regular as shown in Fig. 18(c).

D. Parameter Analysis

In this paper, r is a constant parameter that is used to control the local region size. It should be noted that the fitting function is constructed in the local region. A local region size that is too small easily leads to overfitting. That is, local regions of a smaller size capture little intensity information, so that the estimated fitting function cannot discriminate the object or background pixels. On the contrary, a local region size that is too big can lead to underfitting. Since the larger sized local regions include too much intensity information, the fitting function cannot accurately extract the effective information. While the images that have a larger size and higher resolution ratio are processed, the greater r is used to select the larger local region; a greater number of details are necessary to approximate and fit the image intensity. Here, we give an example to explain the size setting. In Fig. 19, three images with different resolution ratios and sizes are separately segmented: Fig. 19 (a) 150×230, Fig. 19 (b) 321×481 and Fig. 19 (c) 400×600. To accurately segment the three images in Fig. 19, the parameter settings are set as follows: $r = 6$ in Fig. 19(a), $r = 20$ in 19(b) and $r = 24$ in 19(c). Therefore, we argue that the images that are larger or that have a higher resolution ratio are needed to set a bigger r.

V. CONCLUSIONS

In this paper, we proposed a LATE method to segment images with intensity inhomogeneity that is based on first-order Taylor expansion. Unlike existing models, the first-order Taylor expansion is first utilized to approximate and describe intensity inhomogeneity images. The local statistical intensity information and the variation degree information of intensity inhomogeneity are jointly incorporated into the proposed model, so it is a nonlinear description method and can better approximate images with severe intensity inhomogeneity. The LATE method can be utilized to solve nonconvex optimization of the fitting function. Meanwhile, the local contrast of images is also enhanced due to the introduction of the variation degree of intensity inhomogeneity. Many experiments on synthetic and real images have been conducted that clearly show the effectiveness of the proposed LATE method.

REFERENCE

[1] M. Styner, C. Brechbuhler, G. Szckely, G. Gerig, Parametric estimate of intensity inhomogeneities applied to MRI, IEEE Transactions on Medical Imaging, 19(3), pp. 153 - 165, 2000

[2] U. Vovk, F. Pernus, and B. Likar, “A review of methods for correction of intensity inhomogeneity in MRI,” IEEE Trans. Med. Imaging, vol. 26, no. 3, pp. 405–421, Mar. 2007.

[3] Z. Hou, “A review on MRI image intensity inhomogeneity correction,” Int. J. Biomed. Imag., vol.2006, pp.1-11, 2006.

[4] C. Li, C. Gatenby, L. Wang, and J. Gore, “A robust parametric method for bias field estimation and segmentation of MR images,” in Proc. IEEE Conf. Comput. Vision Pattern Recog., 2009, pp. 218–223.

[5] V. Caselles, R. Kimmel, and G. Sapiro, “Geodesic active contours,” Int. J. Comput. Vis., vol. 22, no. 1, pp. 61–79, 1997.

[6] L. Vese and T. Chan, “A multiphase level set framework for image segmentation using the Mumford and Shah model,” Int. J. Comput. Vis., vol. 50, no. 3, pp. 271–293, 2002.

[7] B. Wang, X. Gao, D. Tao, and X. Li, “A nonlinear adaptive level set for image segmentation,” IEEE Trans. Cybern., vol. 44, no. 3, pp. 418–428, Mar. 2014.

[8] X. Gao, B. Wang, D. Tao, and X. Li, “A relay level set method for automatic image segmentation,” IEEE Trans. Syst., Man, Cybern. B, Cybern., vol. 41, no. 2, pp. 518–525, Apr. 2011.

[9] T. Chan, L. Vese, “Active contours without edges,” IEEE Trans. Image-Process., vol. 10, no. 2, pp. 266–277, 2001.

[10] S. Osher and J. A. Sethian, “Fronts propagating with curvaturedependent speed: Algorithms based on Hamilton–Jacobi formulations,” J. Comput. Phys., vol. 79, no. 1, pp. 12–49, 1988.

[11] C. Li, C. Kao, J. C. Gore, and Z. Ding, “Minimization of region-scalable fitting energy for image segmentation,” IEEE Trans. Image-Process., vol. 17, no. 10, pp. 1940–1949, 2008.

[12] C. Li, C. Kao, J. Gore, and Z. Ding, Implicit Active Contours Driven by Local Binary Fitting Energy, IEEE Conference on Computer Vision and Pattern Recognition., pp.1–7, 2007.

[13] S. Lankton and A. Tannenbaum, “Localizing region-based active

contours," IEEE Trans. Image-Process., vol. 17, no. 11, pp. 2029–2039, 2008.

[14] K. Zhang, H. Song, and L. Zhang., Active Contours Driven by Local Image Fitting Energy., Pattern recognition, vol.43, issue 4, pp. 1199-1206, April 2010.

[15] C. Darolti, A. Mertins, C. Bodensteiner, and U. Hofmann, "Local Region Descriptors for Active Contours Evolution, " IEEE Transactions on Image-Processing., vol.17, no.12, pp.2275–2288, 2008.

[16] L. Wang, L. He, A. Mishra, C. Li. "Active Contours Driven by Local Gaussian Distribution Fitting Energy," Signal Processing, 89(12), pp. 2435-2447,2009.

[17] Z.X. Ji, Y. Jia, Q.S. Sun, et al. Active contours driven by local likelihood image fitting energy for image segmentation. Inf. Sci., 301, pp. 285–304, 2015

[18] K.Sum and P.Cheung, "Vessel extraction under non-uniform illumination: A level set approach," IEEE Trans.Biomed. Eng., vol.55, no.1,pp.358-360, Jan.2008.

[19] B. Wang, X.-B. Gao, et al. "A Unified Tensor Level Set for Image Segmentation,". IEEE Trans. on System, Man, and Cybernetics Part B: Cybernetics, Vol. 40, No.3, pp.857-867, 2010.

[20] X. Wang, D. Huang and H. Xu, "An efficient local Chan-Vese model for image segmentation", Pattern Recognition, 43(3), pp.603-618, 2010.

[21] X.F. Wang, H. Min, L. Zou, Y.G. Zhang, A novel level set method for image segmentation by incorporating local statistical analysis and global similarity measurement. Pattern Recognition, 48(1),pp.189-204, 2015.

[22] H. Min, W. Jia, X.F. Wang, et al. "An intensity-texture model based level set method for image segmentation," Pattern Recognition, 48(4): 1547-1562, 2015.

[23] L. Dai, J. Ding, J. Yang, "Inhomogeneity-embedded active contour for natural image segmentation," Pattern Recognition, 48(8): 2513-2529,2015.

[24] C. Li, R. Huang, Z. Ding, C. Gatenby, D. Metaxas, and J. C. Gore, "A Level Set Method for Image Segmentation in the Presence of Intensity Inhomogeneities with Application to MRI," IEEE Transactions on Image-Processing, vol.20, no.7, pp.2007–2016, 2011.

[25] C. Bishop. Pattern Recognition and Machine Learning. Springer, Aug. 2006.

[26] H. Zhang, X. Ye and Y. Chen "an efficient algorithm for multiphase image segmentation with intensity bias correction," IEEE Transactions on Image-Processing 22(10), pp.3842–3851, 2013.

[27] Y. Zhang, M. Brady, and S. Smith, "Segmentation of brain MR images through a hidden Markov random field model and the expectation maximization algorithm," IEEE Trans. Med. Imag., vol. 20, no. 1, pp. 45–57, Jan. 2001.

[28] C. Li, X. Wang, S. Eberl, M. Fulham, D. Feng: Robust Model for Segmenting Images With/Without Intensity Inhomogeneities. IEEE Transactions on Image-Processing, 22(8), pp.3296-3309, 2013.

[29] Y. Duan, H. Chang, W. Huang, J. Zhou, Z. Lu and C. Wu, "The L0 regularized Mumford-Shah model for bias correction and segmentation of Medical images", IEEE Transactions on Image-Processing, 24(11): 3927-3938, 2015.

[30] K. Zhang, Q. Liu, H. Song, and X. Li., A Variational Approach to Simultaneous Image Segmentation and Bias Correction., IEEE Trans. Cybernetics, 45(5), pp. 1426-1437, 2015.

[31] K. Zhang, L. Zhang, K. M. Lam, and D. Zhang, A Level Set Approach to Image Segmentation with Intensity Inhomogeneity., IEEE Trans. Cybernetics, 46(2), pp.546-557, 2016.

[32] Y. Zhang, L. Xu, X. Ji, and Q. Dai, A Polynomial Approximation Motion Estimation Model for Motion-Compensated Frame Interpolation, IEEE Transactions on Circuits and Systems for Video Technology, 26(8), 2016.

[33] Http://brainweb.bic.mni.mcgill.ca/brainweb/.

[34] C. Li, J.C. Gore, and C. Davatzikos, "Multiplicative intrinsic component optimization (MICO) for MRI bias field estimation and tissue segmentation", Magnetic Resonance Imaging, vol. 32 (7), pp. 913-923, 2014.

[35] http://www.wisdom.weizmann.ac.il/~vision/Seg_Evaluation_DB/1obj/index.html

[36] https://www2.eecs.berkeley.edu/Research/Projects/CS/vision/grouping/resources.html